Optics and Spectroscopy, Vol. 94, No. 3, 2003, pp. 469–475. Translated from Optika i Spektroskopiya, Vol. 94, No. 3, 2003, pp. 514–521.

LASERS AND THEIR APPLICATIONS

Radiative Characteristics of a Two-Section Laser Structure Based on a δ-Doping Superlattice

D. V. Ushakov*, V. K. Kononenko, and I. S. Manak***

**Belarussian State University, Minsk, 220050 Belarus*

***Stepanov Institute of Physics, National Academy of Sciences of Belarus, Minsk, 220072 Belarus*

e-mail: lavik@dragon.bas-net.by

Received August 7, 2002

Abstract—Spectral characteristics of a two-section laser structure with δ-doping active regions are studied theoretically. The wide range of tuning of the lasing wavelength is primarily related to specific characteristics of the gain spectra of *n–i–p–i* crystals: the dependence of the effective band-gap width of the superlattice on the level of excitation, the character of variation of the overlap integrals of the electron and hole wave functions, and broadening of the electronic spectra due to fluctuations of the electrostatic potential. Depending on the pumping currents in sections of the laser structure, the lasing wavelength can be tuned over a wide spectral range of the IR region in regimes of cw lasing, the transient regime, and the regime of regular pulsations. In the regime of self-sustaining pulsations, lasing is also possible at two wavelengths spaced well apart. © *2003 MAIK "Nauka/Interperiodica".*

INTRODUCTION

Systems of optical information processing and spectral analysis need sources of laser emission tunable in a wide spectral range. Great possibilities for controlling the emission wavelength are displayed by injection lasers, which are convenient in operation [1]. In particular, laser diodes based on nonuniformly pumped asymmetric quantum-well heterostructures made it possible to realize quasi-cw spectral tuning of laser emission to within 22 nm in the range of 8 μm [2]. Wavelength tuning under nonuniform excitation of multisection lasers is based on variation of the cavity finesse, which entails a change in position of the gain maximum.

In choosing parameters of asymmetric quantum-well laser heterostructures, one can control, in a wide range, the gain spectrum and, correspondingly, the tuning curves of sources for diode laser spectroscopy [3]. On this basis, one can also create new generators of regular light pulses for integral optics, rangefinding, detector calibration, monitoring of information storage, and automatic control.

Dynamic tuning of the pulsed-laser emission spectrum (sweeping) is most efficient for active media with wide, homogeneously broadened gain bands [4]. In such cases, a wide range of spectral tuning is ensured at high radiance of the laser emission with smooth variation of the integrated power. Sweep lasing has been achieved in such active media as dye solutions [5] and crystals with color centers [6]. Pulsed lasers based on these active media, due to the short durations of lasing (of the order of 10^{-8}–10^{-5} s), require rates of controlling the selective-loss spectrum of the cavity that are higher than 10^3 cm^{-1}/μs. An increase in the rate of sweeping and the search for new principles of dynamic tuning of the lasing spectrum are also important from the viewpoint of development of rapid methods of spectroscopic measurements.

Among broadband laser systems are structures based on doping superlattices, or *n–i–p–i* crystals [7, 8]. The power and spectral characteristics of these systems are readjusted due to transformation of the electronic spectrum in the process of excitation and emission [9]. Considerable opportunities arise under nonuniform excitation of a two-section laser structure with a δ-doped *n–i–p–i* crystal [10–12]. In this paper, we discuss various modes of operation of such lasers and analyze the laser wavelength-sweeping process in a wide range of the IR spectrum.

TUNING OF THE GAIN SPECTRUM

Tuning of the energy and spectral characteristics in doping semiconductor superlattices is mainly conditioned by variations of the depth of the potential relief ($2\Delta V$) and, correspondingly, the effective width of the band gap (E_g') with increasing excitation power. Thus, to achieve a wide tuning range, it is necessary to choose structures with high values of $2\Delta V$ and short superlattice periods. The values of $2\Delta V$ in δ-doping *n–i–p–i*-crystals, compared with ordinary doping superlattices (with the same periods), are larger [7, 8]. In addition, due to the larger overlap of electron and hole wave functions in the structures with δ-doping layers, a fairly high gain may be achieved at relatively low levels of excitation of the crystal [13, 14].

0030-400X/03/9403-0469$24.00 © 2003 MAIK "Nauka/Interperiodica"

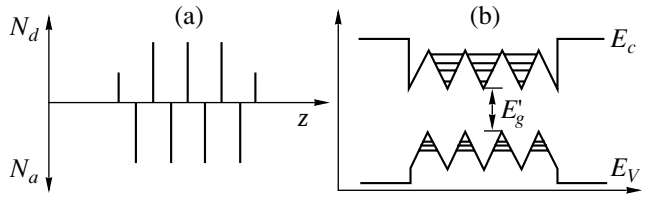

Fig. 1. The doping profiles $N_d(z)$ and $N_a(z)$ (a) and band diagram (b) of a GaAs-based δ-doping superlattice. Also shown are the energy levels of electrons and heavy holes, as well as the band edges of the emitters E_c and E_V.

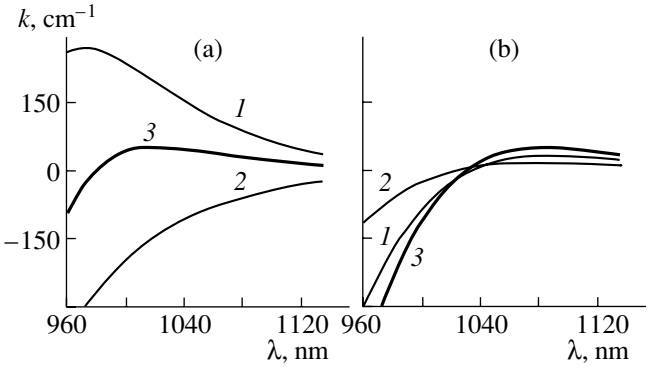

Fig. 2. The gain spectra in the first $r_1k_1(\lambda)$ (*1*) and second $r_2k_2(\lambda)$ (*2*) sections and the spectra of the total gain $k(\lambda)$ (*3*) for $r_1 = 0.7$ and $r_2 = 0.3$ and different two-dimensional electron concentrations: (a) $n_1 = 8.2 \times 10^{12}$ cm^{-2}, $n_2 = 0.5 \times 10^{12}$ cm^{-2} and (b) $n_1 = n_2 = 4.9 \times 10^{12}$ cm^{-2}.

Now consider a GaAs-based four-period δ-doping *n–i–p–i* superlattice with equal surface concentrations of donor and acceptor impurities ($N_d d_n = N_a d_p = 10^{13}$ cm^{-2}) and with an undoped region with width $d_i = 9$ nm. The band diagram of such a structure is shown schematically in Fig. 1. The superlattice period is of the order of $d = d_n + d_p + 2d_i \approx 20$ nm. In the laser structure, two nonuniformly excited sections can be distinguished, with one (or both) of them being capable of amplifying the light.

The calculation of the potential-energy profile, quantum-dimensional energy levels, and wave functions of electrons and holes was performed by solving numerically and self-consistently the Schrödinger and Poisson equations with allowance for charge-carrier screening effects, band-gap narrowing, and impurity density fluctuations [9]. The gain spectrum and the rate of spontaneous radiative recombination were calculated using the model of direct transitions and Gaussian tails of the density of states. The procedure of accounting for the effects of broadening of the electronic spectrum and calculation of the emission spectra of the doping superlattices is described in more detail in [15].

The tuning range of the lasing wavelength for a given gain at the maximum of the resulting gain spectrum $k(\lambda)$ of a two-section laser depends on the values of the relative lengths of the nonuniformly excited parts of the active region r_1 and r_2 ($r_1 + r_2 = 1$),

$$k(\lambda) = r_1k_1(\lambda) + r_2k_2(\lambda),$$

where k_1 and k_2 are the gain factors of the first and second sections. In this case, the resulting gain factor $k(\lambda)$ at the maximum of the gain spectrum should be equal, in the cw lasing mode, to the loss factor k_l.

Figure 2 shows the gain spectra at different levels of excitation of the laser structure [10]. For a given loss factor, the greatest lasing wavelength is reached at equal two-dimensional electron densities n_1 and n_2, respectively, in the first and second sections of the structure (Fig. 2b). In this case, the light is amplified in both laser sections. As the electron concentration in the amplifying section increases, the excitation level of the second section [to meet the threshold condition $k_{max}(\lambda) = k_l$ should become lower and the wavelength at the maximum of the resulting gain spectrum decreases.

The tuning range of the emission wavelength is limited by the greatest admissible value of the density of the injection current j_{max} in the amplifying section of the diode. For a specified j_{max}, a greater tuning range of the emission wavelength can be achieved by increasing the length of the amplifying section [10]. As seen from Fig. 3a, for $j_{max} \approx 300$ A/cm^2 with $r_1 = 0.5$, 0.6, and 0.7, the tuning range equals 33, 48, and 63 nm, respectively.

It is noteworthy that, at large values of r_1, for tuning the maximum of the gain spectrum toward shorter wavelengths, the excitation levels of the absorbing section should be sufficiently low and, correspondingly, the radiative lifetimes of nonequilibrium current carriers prove to be rather long (up to 1 μs and longer; Fig. 3b). In this case, the lasing is achieved at low densities of the pumping current in the absorbing section of the diode (below 0.1 A/cm^2). To eliminate the effects of saturation in the absorbing section and the subsequent changes in the gain spectrum, it is necessary to reduce the effective lifetime of the nonequilibrium carriers in this section with a corresponding increase in the current.

This can be done by introducing additional structural defects through ion implantation or irradiation by fast particles [16]. Heavy-ion irradiation renders the material amorphous along the ion tracks and, at small irradiation doses, creates in the semiconductor matrices local regions with a sufficiently high nonradiative recombination rate. In particular, the irradiation of GaAs with high-energy oxygen ions creates an efficient channel of nonradiative recombination, which decreases the electron lifetime down to several picoseconds for irradiation doses above 10^{12} cm^{-2} [17, 18]. It has also been noted that implantation does not noticeably change the structure and shape of luminescence

bands and does not induce new emission lines. However, irradiation by electrons affects the photoluminescence spectra of GaAs [19]. A decrease in the current-carrier lifetime in a two-section laser diode can also be achieved at a sufficiently high potential gradient [20].

THE STABILITY OF STEADY-STATE LASING

The lasing dynamics of a two-component injection laser, with emission that propagates along the waveguide part of the structure passing successively through regions of the active layer with different levels of excitation, is described, in the single-mode approximation, by the following system of rate equations [21]:

$$\frac{dn_1}{dt} = \frac{j_1}{ed} - \frac{R_1}{\eta_1} - v_g G_1 S,$$

$$\frac{dn_2}{dt} = \frac{j_2}{ed} - \frac{R_2}{\eta_2} - v_g G_2 S, \qquad (1)$$

$$\frac{dS}{dt} = v_g(r_1 G_1 + r_2 G_2 - k_l)S + \beta(r_1 R_1 + r_2 R_2),$$

where j_1 and j_2 are the current densities; R_1 and R_2 are the rates of spontaneous recombination; η_1 and η_2 are the quantum yields of luminescence in sections *1* and *2*; v_g is the group velocity of light in the crystal; $G_1 = k_1/(1 + \varepsilon_1 S)$ and $G_2 = k_2/(1 + \varepsilon_2 S)$ are the mode gain and absorption coefficients in the corresponding sections, respectively; ε_1 and ε_2 are the parameters of nonlinear gain and absorption, respectively; and β takes into account the contribution of spontaneous transitions to the lasing mode. The photon density S and volume concentrations of the current carriers n_1 and n_2 in sections I and II are normalized here to the superlattice period d.

Let us analyze stability of the steady-state solution of the system of equations (1). In view of the smallness of the contribution of spontaneous emission to the lasing mode, we will restrict our analysis to the approximation of self-excitation ($\beta = 0$). To examine the stability by the Lyapunov method, we have to find the roots of the characteristic equation,

$$\begin{vmatrix} -\theta_1 - x & 0 & -v_g G_1(1-\xi_1) \\ 0 & -\theta_2 - x & -v_g G_2(1-\xi_2) \\ v_g r_1 G_1' S & v_g r_2 G_2' S & -\theta_3 - x \end{vmatrix} = 0. \qquad (2)$$

Here, we used the notations $G_i' = \partial G_i(n_i, S)/\partial n_i$, $\theta_i = \partial(R_i/\eta_i)/\partial n_i + v_g G_i' S$, $\xi_i = \varepsilon_i S/(1 + \varepsilon_i S)$, $i = 1, 2$; and

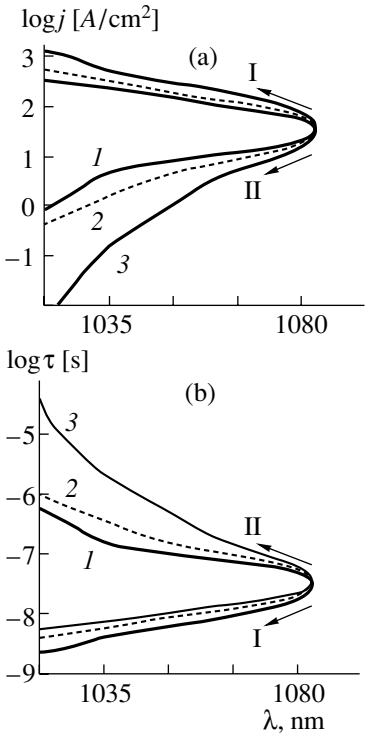

Fig. 3. Variation of the pumping current density j (a) and radiative lifetime τ (b) upon wavelength tuning at the maximum of the resultant gain spectrum for r_1 = (*1*) 0.5, (*2*) 0.6, and (*3*) 0.7. The arrows show the directions of change of j and τ in the first (I) and second (II) laser sections.

$\theta_3 = v_g(r_1\xi_1 G_1 + r_2\xi_2 G_2)$. Calculation of determinant (2) leads to the third-order equation with respect to x:

$$x^3 + x^2(\theta_1 + \theta_2 + \theta_3) + x[F_1 + F_2 + \theta_1\theta_2 + (\theta_1 + \theta_2)\theta_3] + (\theta_1 F_2 + \theta_2 F_1 + \theta_1\theta_2\theta_3) = 0. \qquad (3)$$

Here, $F_i = v_g^2 r_i G_i' G_i(1 - \xi_i)S$ and $i = 1, 2$.

The steady-state solution to the system of equations (1) is stable when two conditions are satisfied. First, the free term of Eq. (3) should be positive and, second, the condition

$$\theta_1\theta_2(\theta_1 + \theta_2) + \theta_1 F_1 + \theta_2 F_2 + \theta_3[F_1 + F_2 + (\theta_1 + \theta_2)(\theta_1 + \theta_2 + \theta_3)] > 0 \qquad (4)$$

should be satisfied.

Analysis of condition (4) shows that the lasing mode becomes unstable and, in particular, self-sustained oscillations arise in the presence of absorption in one of the sections, for example, in section II ($G_2 < 0$). In addition, since the condition of stability (4) involves positive terms with a cubic dependence on the photon density S and negative terms with only a quadratic dependence, it is evident that self-oscillations are absent at a

sufficiently high photon density. At small S, inequality (4) is also valid. Therefore, self-sustained oscillations are possible only within a certain range of pumping current in the sections.

Self-sustained oscillations of the laser emission intensity can be observed if the magnitude of the differential parameter $\partial G_2/\partial n_2$ is large and the absorbing section II is characterized by a small time constant τ_2, which is the inverse of $\partial(R_2/\eta_2)/\partial n_2$. Since the luminescence quantum yield in the absorbing section equals

$$\eta_2 = \frac{R_2(n_2)}{R_2(n_2) + n_2/\tau_{nr2}}, \quad (5)$$

the expression for τ_2 has the form

$$1/\tau_2 = \partial R_2/\partial n_2 + 1/\tau_{nr2}. \quad (6)$$

Here τ_{nr2} specifies the current-carrier lifetime with respect to nonradiative recombination.

As was mentioned above, because of the spacing between the potential wells for electrons and holes, the doping superlattice in the absorbing section exhibits a longer radiative lifetime of the current carriers at the low excitation level needed for lasing in the short-wavelength region of tuning. Thus, with no additional measures for reducing the carrier lifetime in the absorbing section, steady-state lasing is realized only with a reverse current in this section, which corresponds to the reverse bias and to depletion of the carriers. However, when a nonradiative recombination channel is introduced, e.g., by the implantation of oxygen ions, the nonradiative recombination begins to predominate. As a result, the lifetime of the nonequilibrium carriers in the absorbing section drops in accordance with Eq. (6) and the lasing wavelength can be tuned with direct injection current in both sections.

The calculations of the regions of different lasing regimes of the two-section laser, based on an analysis of stability conditions [12], show that, for the nonradiative lifetime $\tau_{nr2} = 1$ ns, the free term of Eq. (3) appears to be positive in a wide range of pumping currents and condition (4) for stable steady-state lasing may be easily satisfied. At $r_1 = 0.7$, the spectral tuning range of the steady-state lasing may reach 30 nm (from 1053 to 1083 nm).

LASING DYNAMICS

Considerable tuning of the lasing wavelength is possible only in the pulsed mode. Dynamic processes in the two-section laser are studied here on the basis of the following system of equations [11, 22]:

$$\frac{dn_i}{dt} = \frac{j_i}{ed} - \frac{R_i(n_i)}{\eta_i} - v_g \sum_j \frac{k_i(n_i, \lambda_j)}{1 + \varepsilon S_{\text{tot}}} S_j,$$
$$\frac{dS_j}{dt} = v_g \sum_i \frac{r_i k_i(n_i, \lambda_j)}{1 + \varepsilon S_{\text{tot}}} S_j - v_g k_l S_j + \beta \sum_i r_i R_i(n_i). \quad (7)$$

The subscript $i = 1, 2$ is related to the first and second sections of the laser. Note that, in the non-stationary regime, several modes are generated, and, thus, a set of photon densities S_j for N modes ($j = 1, \ldots, N$) is present in the system of rate equations. The resultant photon density S_{tot} is determined as a sum of all the modes $S_{\text{tot}} = \sum_j S_j$, and the average value of the wavelength of lasing emission is determined as

$$\lambda_{\text{av}}(t) = \frac{\sum_j \lambda_j S_j(t)}{S_{\text{tot}}(t)}. \quad (8)$$

We also assume, for simplicity, that $\varepsilon_1 = \varepsilon_2 = \varepsilon$. The luminescence quantum yield in the first section η_1 is assumed to be unity, while, in the second part of the diode, η_2 was calculated using Eq. (5).

Analysis of the lasing dynamics showed that, in a two-section laser based on a δ-doping superlattice, one can effect three ways of tuning the emission wavelength. One way is realized in the regime of self-sustained emission pulsations [12]. A regime of persistent pulsations of emission arises when the steady-state solution of the system of rate equations (1) is unstable. The range of pumping currents within which self-modulated pulsations of the emission arise is limited from above by the stability boundary and from below by the threshold currents. The shortest lasing wavelength of self-sustained pulsations of emission is achieved at low currents in the absorbing section j_2. For high values of j_2, the greatest wavelength of persistent pulsations is realized.

Figure 4 shows the time dependences of the electron concentrations in the amplifying (n_1) and absorbing (n_2) sections of the laser and of the total photon density S_{tot} after applying a step of pumping current specifying two different steady-state emission wavelengths of regular pulses. The losses introduced by the absorbing section favor accumulation of the current carriers in the bands. The emission pulse arising bleaches the absorbing section, thus sharply reducing the total losses. As a result, the accumulated inverted population is utilized for generation of a strong emission peak. After quenching of lasing, the population n_1 increases due to injection while the concentration n_2 drops due to nonradiative recombination, and then the process is repeated anew. Figure 4d shows that, as the current in the absorbing

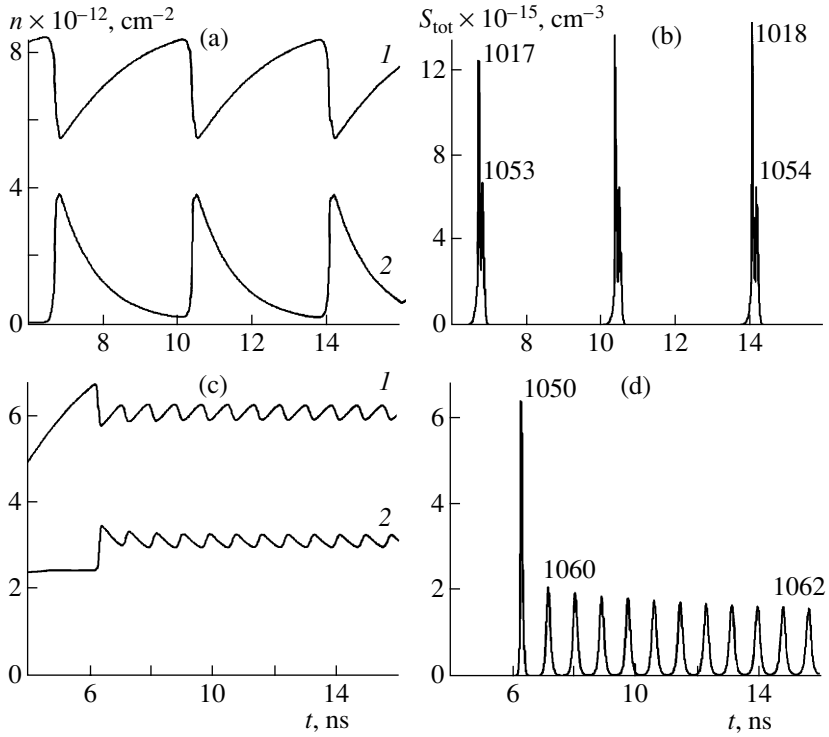

Fig. 4. Regime of self-sustained emission pulsations in a two-section laser. (a), (c) The time dependence of a two-dimensional concentration of electrons n in the first (*1*) and second (*2*) laser sections; (b), (d) time dependence of the total photon density S_{tot}. Current densities in the sections: (a, b) $j_1 = 300$ A/cm^2 and $j_2 = 10$ A/cm^2; (c, d) $j_1 = 200$ A/cm^2 and $j_2 = 390$ A/cm^2. The figures on the peaks of $S_{tot}(t)$ correspond to the average wavelength of the laser emission pulses λ_{av} (in nm); $k_l = 50$ cm^{-1}, $\tau_{nr2} = 1$ ns, $\varepsilon = 5 \times 10^{-18}$ cm^3, and $r_1 = 0.7$.

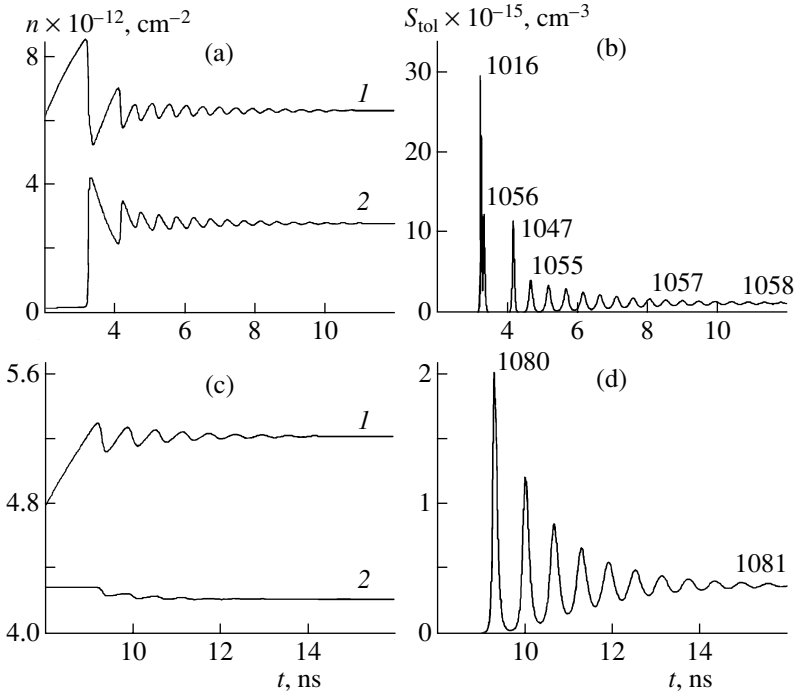

Fig. 5. (a, c) Time dependence of the two-dimensional electron concentration n in the first (*1*) and second (*2*) laser sections; (b, d) time dependence of the total photon density $S_{tot}(t)$. Current densities in the sections: (a, b) $j_1 = 500$ A/cm^2, $j_2 = 30$ A/cm^2; (c, d) $j_1 = 100$ A/cm^2 and $j_2 = 700$ A/cm^2. The figures on the peaks of $S_{tot}(t)$ correspond to the average wavelength of the laser emission pulses λ_{av} (in nm); $k_l = 50$ cm^{-1}, $\tau_{nr2} = 1$ ns, $\varepsilon = 5 \times 10^{-18}$ cm^3, and $r_1 = 0.7$.

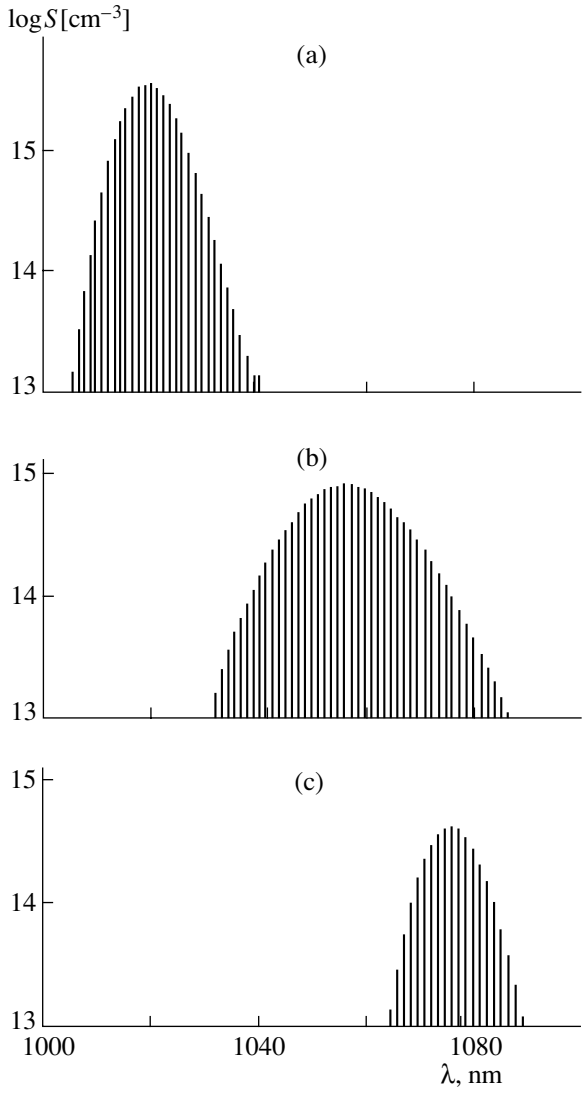

Fig. 6. Mode composition of the emission $S(\lambda)$ at different times t = (a) 3.19, (b) 3.26, and (c) 3.47 ns; j_1 = 500 A/cm^2, j_2 = 20 A/cm^2, k_l = 50 cm^{-1}, $\varepsilon = 5 \times 10^{-18}$ cm^3, and r_1 = 0.7.

section of the laser increases, the repetition rate and amplitude of the laser emission pulses decrease. Thus, the lasing wavelength can be tuned in the range of 1017–1062 nm in a dynamic regime by adjusting the current in the sections.

Note that, in the regime of self-sustained pulsations in a two-section laser based on a doping superlattice, the generation of twinned spectrally spaced pulses is possible (Fig. 4b). The appearance of a long-wavelength emission pulse immediately after a first powerful short-wavelength pulse is explained in the following way [12]. After the end of the first emission pulse, the density of nonequilibrium carriers in the absorbing section increases while that in the amplifying section drops. The resultant gain factor in the short-wavelength region appears to be small, with its maximum shifted toward longer wavelengths. If the total gain factor in a certain wavelength range turns out to be higher than the loss factor, then the lasing of a long-wavelength emission pulse occurs. In this case, the absorbing section introduces a kind of time-dependent "dynamic losses" ($r_2 k_2(\lambda, t) < 0$) [23]. For the laser structure under study in the regime of self-sustained pulsations of emission, the lasing of twinned pulses occurs at the wavelengths of 1018 and 1054 nm. The pulse width, in this case, is approximately equal to 30 ps.

Another way of tuning of the lasing wavelength in a two-section laser based on a δ-doping superlattice is related to changes of the wavelength in the first relaxation peak upon variation of the pumping currents in the first and second sections of the diode [11]. As follows from calculations, the greatest range of spectral tuning in the first relaxation peak is achieved for current densities corresponding to the range of the stable steady-state lasing.

The shortest tuning wavelength is realized at low currents in the absorbing section of the structure and at high currents in the amplifying section. In the absence of a nonradiative recombination channel ($\tau_{nr} \longrightarrow \infty$), the longest wavelength in the first relaxation peak is reached at equal current densities in both laser sections, while, when nonradiative centers are introduced, the densities of injection currents in the sections under these lasing conditions become different.

The dynamics of variation of the two-dimensional electron densities in the first and second laser sections and of the total photon density upon application of the pumping current step is shown in Fig. 5. As is seen, the average wavelength in the first relaxation peak may vary within the wavelength range 1016–1080 nm in dependence on the amplitude of pumping currents. Similar estimates made for two-section lasers with an active medium based on bulk semiconductors yield a tuning range of less than 10 nm [22].

As is seen from Fig. 5b, the laser may generate a succession of pulses with wavelength increasing from 1016 to 1058 nm, similarly to a sweep laser [4–6, 23], which may be considered as one more way to tune the lasing wavelength [11]. A wider range and smoother tuning of the wavelength in time can be obtained without introducing an additional recombination channel into one of the laser sections [11]. In particular, for a luminescence quantum yield in the absorbing laser section $\eta_2 \approx 1$, the tuning range of the lasing wavelength may reach 73 nm (from a wavelength of 1007 nm in the first relaxation peak to 1080 nm in the steady-state regime). The tuning range also depends on the relative lengths of the laser sections. For given injection currents in the sections, the wavelength tuning range varies from 69 nm at r_1 = 0.6 to 63 nm at r_1 = 0.7 and reaches its maximum, of the order of 73 nm, at r_1 = 0.65.

Figure 6 shows the mode composition of the emission at different times. In the calculations, the intermode spacing was assumed to be 1.4 meV, which cor-

responded to the cavity length ~100 μm. The set of lasing modes is seen to vary noticeably in time. The average values of the lasing wavelengths at the moments t = 3.19, 3.26, and 3.47 ns are equal, respectively, to 1017, 1055, and 1075 nm.

CONCLUSIONS

Thus, depending on the pumping currents in the sections of a laser structure based on a δ-doping superlattice, one can obtain tuning of the emission wavelength in a wide spectral range in the regimes of steady-state lasing, transient process, and regular pulsations. In the regime of self-sustained pulsations, laser emission at two widely spaced wavelengths is also possible. In GaAs-based structures, the tuning range in the vicinity of 1 μm reaches 70 nm.

ACKNOWLEDGMENTS

The authors are grateful to A.A. Afonenko for discussions of the results and assistance. This study was supported by the Belarussian National Foundation for Basic Research.

REFERENCES

1. A. I. Nadezhdinskii and A. M. Prokhorov, Proc. SPIE **3724**, 2 (1992).
2. S. Ikeda, A. Shimizu, Y. Sekiguchi, *et al.*, Appl. Phys. Lett. **55**, 2057 (1989).
3. V. K. Kononenko, A. A. Afonenko, I. S. Manak, and S. V. Nalivko, Opto-Electron. Rev. **8**, 241 (2000).
4. S. P. Anokhov, T. Ya. Marusiĭ, and M. S. Soskin, *Tunable Lasers* (Radio i Svyaz', Moscow, 1982).
5. F. V. Karpushko and G. V. Sinitsyn, Pis'ma Zh. Tekh. Fiz. **3** (8), 337 (1977) [Sov. Tech. Phys. Lett. **3**, 137 (1977)].
6. F. V. Karpushko and N. A. Saskevich, Pis'ma Zh. Tekh. Fiz. **6** (5), 264 (1980) [Sov. Tech. Phys. Lett. **6**, 114 (1980)].
7. E. F. Schubert, Surf. Sci. **228**, 240 (1990).
8. E. F. Schubert, Opt. Quantum Electron. **22**, S141 (1990).
9. V. K. Kononenko, I. S. Manak, and D. V. Ushakov, Proc. SPIE **3580**, 10 (1998).
10. D. V. Ushakov, A. A. Afonenko, and I. S. Manak, in *Proceedings of IV International Conference on Laser Physics and Spectroscopy* (Grodno, 1999), Part 1, p. 125.
11. D. V. Ushakov, A. A. Afonenko, and I. S. Manak, Lith. Phys. J. **39**, 361 (1999).
12. D. V. Ushakov, V. K. Kononenko, and I. S. Manak, in *Proceedings of 2nd International Conference on Transparent Optical Networks* (Gdansk, 2000), p. 41.
13. D. V. Ushakov and V. K. Kononenko, *Physics, Chemistry and Application of Nanostructures* (World Sci., Singapore, 1997), pp. 121–124.
14. D. V. Ushakov, V. K. Kononenko, and I. S. Manak, *Nonlinear Phenomena in Complex Systems* (Minsk, 1999), pp. 144–151.
15. V. V. Ushakov, V. K. Kononenko, and I. S. Manak, Zh. Prikl. Spektrosk. **66**, 711 (1999).
16. F. P. Korshunov, G. B. Gatal'skiĭ, and G. M. Ivanov, *Radiation Effects in Semiconductor Devices* (Nauka i Tekhnika, Minsk, 1978).
17. Zh. I. Alferov, A. B. Zhuravlev, E. L. Portnoĭ, and N. M. Stel'makh, Pis'ma Zh. Tekh. Fiz. **12** (18), 1093 (1986) [Sov. Tech. Phys. Lett. **12**, 452 (1986)].
18. A. B. Zhuravlev, V. A. Marushchak, E. L. Portnoĭ, *et al.*, Fiz. Tekh. Poluprovodn. (Leningrad) **22**, 352 (1988) [Sov. Phys. Semicond. **22**, 217 (1988)].
19. F. P. Korshunov, A. V. Mudryĭ, A. I. Patuk, and I. A. Shakin, Zh. Prikl. Spektrosk. **64**, 122 (1997).
20. P. P. Vasil'ev and I. S. Goldobin, USSR Inventor's Certificate No. 1614056, Otkrytiya, Izobret., No. 46, 230 (1990).
21. L. A. Rivlin, A. T. Semenov, and S. D. Yakubovich, *Dynamics and Emission Spectra of Semiconductor Lasers* (Radio i Svyaz', Moscow, 1983).
22. A. A. Afonenko, Candidate's Dissertation in Physics and Mathematics (Belorus. Gos. Univ., Minsk, 1997).
23. A. V. Kazberuk, V. F. Karpushko, and G. V. Sinitsin, Zh. Prikl. Spektrosk. **33**, 561 (1980).

Translated by V. Zapasskiĭ